Carpathian Journal of Earth and Environmental Sciences, February 2020, Vol. 15, No. 1, p. 113 - 125; DOI:10.26471/cjees/2020/015/114

DIFFERENTIAL INTERLAYER DEFORMATION AND ITS SIGNIFICANCE FOR HYDROCARBON ACCUMULATION IN THE TAZHONG AREA, TARIM BASIN, NW CHINA

Fei NING[1,2,3], Guangzhou MAO[3], JinbiaoYUN[1,2], Zhongpei ZHANG[2] & Li DONG[2]

*[1.]Laboratory of Structural and Sedimentological Reservoir Geology, Exploration & Production Research Institute, SINOPEC, Beijing, China, 100083; *Corresponding author email address: ningfei037@aliyun.com*

[2.] Exploration& Production Research Institute, SINOPEC, Beijing, China, 100083;

[3.] Shandong Provincial Key Laboratory of Depositional Mineralization & Sedimentary Minerals, Shandong University of Science and Technology, Qingdao, China, 266590

Abstract: Differential interlayer deformation and structural coupling are the major characteristics of tectonic deformation in the Tazhong area. In this paper, the geometric characteristics and deformation mechanisms of faults in the Tazhong area were analyzed through a detailed interpretation of seismic sections, analysis of rock mechanical tests and application physical analog methods to gain a better understanding of the pattern of structural deformation in the Tazhong area. The deformation mechanism revealed in this paper also provides insights that will benefit the exploration of large hydrocarbon reserves in this area. It is proposed that the structural coupling effect in the area has typical "superimposed" characteristics. Deformation in the deep and intermediate layers and in the shallow layers is independent but exhibits certain similarities. The sandbox model of the study area revealed that there is a strong correlation between preexisting basement structures (basement uplifts and faults) and faults in the overlying layers. Because of the combined effects of basement structures and decollement layers, a fault is more likely to slip above the preexisting basement structures, thereby forming "superimposed" faults. Although the structural coupling effect can improve the diversity of trap styles and contributes to vertical hydrocarbon migration, the faulting associated with structural coupling also destroys the cap rocks, which is detrimental to hydrocarbon preservation.

Keywords: structural coupling; fault styles; differential structural deformation; mechanism of deformation; Tazhong area; Tarim Basin

1. INTRODUCTION

Differential interlayer deformation is a common form of structural coupling in geological evolution (Uydea, 1983; Klein, 1987; Beaumont et al., 1992; Kay & Mahlburg 1993; Guo, et al., 2003). Basin-mountain coupling is defined by the interaction between continental plates and the structural differences on both sides of an active continental margin resulting from the tectonic movement of ocean and continental crusts (Bally, 1975, Hsu, 1988, Li et al., 2003; Bashir et al., 2013). However, inside a basin, especially for multiphase superimposed basins, there are universal delamination deformation styles that reflect the interconnectedness of different structural units (Schlische et al., 1996; Kim & Sanderson, 2005; Bonini et al., 2016). Differential structural deformation occurs in different structural layers for various reasons, such as changes in the multistage stress field, changes in various deforming media and changes in the multidirectional boundary conditions caused by multiphase tectonic evolution. In particular, the effect of delamination deformation leads to later structural stacking and reorganization in superimposed basins, inevitably influencing hydrocarbon accumulation and complicating its process (Xiao et al., 2000; Jin, 2005; Tang et al., 2009). In the Tarim Basin, the lower Cambrian gypsum salt layer, which is widely developed in the

central uplift, serves as the regional decollement layer and exerts considerable control over the structural deformation of the overlying formations. Extensive previous studies have mainly focused on geometric styles (Li et al., 2008; Li et al., 2013; Wu et al., 2012; Yang et al., 2013) and structural evolution (Zhang et al., 2002; Li et al., 2009; Yu et al., 2010; Guan et al., 2011), as well as hydrocarbon accumulation (Yang et al., 2007; Xiang et al., 2010; Pang et al., 2013, Liu et al., 2015), among other aspects. However, few systematic studies have focused on the characteristics and mechanisms of deformation controlled by the deep gypsum salt layer in the Tazhong area. Differential interlayer deformation not only impacted the development of structural traps and stratigraphic-lithologic traps but also greatly influenced hydrocarbon migration and the development of source rocks and reservoirs. The characteristics and mechanisms of differential interlayer deformation are analyzed in this paper. The petroleum significance in the geological context is also discussed through detailed interpretation of seismic data, rock mechanics tests and physical analog modeling. The results presented herein provide new insights that will improve the reliability of exploration and reduce exploration costs in the Tazhong area.

For centuries, sandbox models have been used to investigate structural evolution on length and time scales suitable for easily repeatable laboratory experiments (Hall, 1815; Graveleau et al., 2012). Utilizing controlled displacements and properly scaled material properties (McClay & Scott, 1991), analog models provide quantitative data on fault system evolution, including the evolving displacement field and the basal conditions required to deform the sand body. Sandbox motors that estimate stress in situ (Nieuwland et al., 2001) or along their moving wall (Cruz et al., 2010; Cubas et al., 2010; Souloumiac et al., 2012) permit direct observations of the formation process during fault evolution. Similarly, direct fault evolution records the process of complicated structural styles, and the data can be used to reveal the mechanism of differential interlayer deformation.

2. GEOLOGICAL SETTING

The Tazhong area is located at the east-central region of the central uplift of the Tarim Basin. It is bounded to the north by the Manjiaer depression, to the west by the Awati depression and to the south by the Tanggubasi depression. The formation and evolution of the Tazhong paleo-uplift, which remained stable during the Caledonian orogeny (Zhang et al., 2002), has been influenced by the structural evolution of the Tarim Basin. The structure of this region as a whole is NW-SE trending. Four groups of faults are present in the region: Tazhong I, Tazhong 10, Tazhong II and the southern edge fault zone (from north to south). These fault zones form a broom-like fault belt that exhibits obvious zonation characteristics in the horizontal plane, as shown in figure 1c. The Tazhong 10 fault belt and the Tazhong II fault belt, which are in the center of the paleo-uplift, are associated with anticline and faulted block structures in profile, forming uplifted fault block structures after later structural denudation and sedimentary compaction. Numerous faults in the horizontal plane are vergent from east to west, forming a narrowing eastward structural framework.

The stratum development in the Tazhong area is characterized entirely by deposition. This area is located in the central area of the Tarim Basin, where strata are well developed. In the main part of the structural high, the Upper Ordovician Qiaerbake Formation and the Middle Ordovician Yijianfang Formation are absent. However, in this area, Paleozoic, Mesozoic and Cenozoic units are all well developed.

The Cambrian units host the major oil resources and are widely distributed in the Tarim Basin (Fig. 2). The lithology of the Cambrian units is primarily shallow marine platform carbonate rocks that are dominated by dolomite. As vital detachment zones, salt layers play an important role in the differential interlayer deformation of the Tazhong area. These salt layers consist of the Lower Cambrian Wusonggeer Formation and the Middle Cambrian Shayilike and Awatage Formations. Well data from the western central uplift indicate that the Lower Cambrian Wusonggeer Formation (∈1w) is composed of colorless salt, gypsum-bearing salt, dolomitic mudstone and gray dolomite, and its thickness ranges from 160 to 300 m. The depositional environment is interpreted as a lagoon on an evaporative platform. The sedimentary environment of the Middle Cambrian Shayilike Formation (∈2s) is interpreted as a tidal flat on a restricted platform. Well data indicate that this formation is composed of gray medium- to thin-layered dolomicrite, limey dolostone, limestone and dolomitic limestone, and its thickness ranges from 30 to 52 m. An outcrop of the Middle Cambrian Awatage Formation reveals that this formation is composed of gypsum salt with a thickness ranging from 143 to 261 m. The main lithology is brick red and light gray medium- to thin-banded chert and shaly dolomite, dolomitic limestone, arenaceous dolomite, shale and pelitic siltstone.

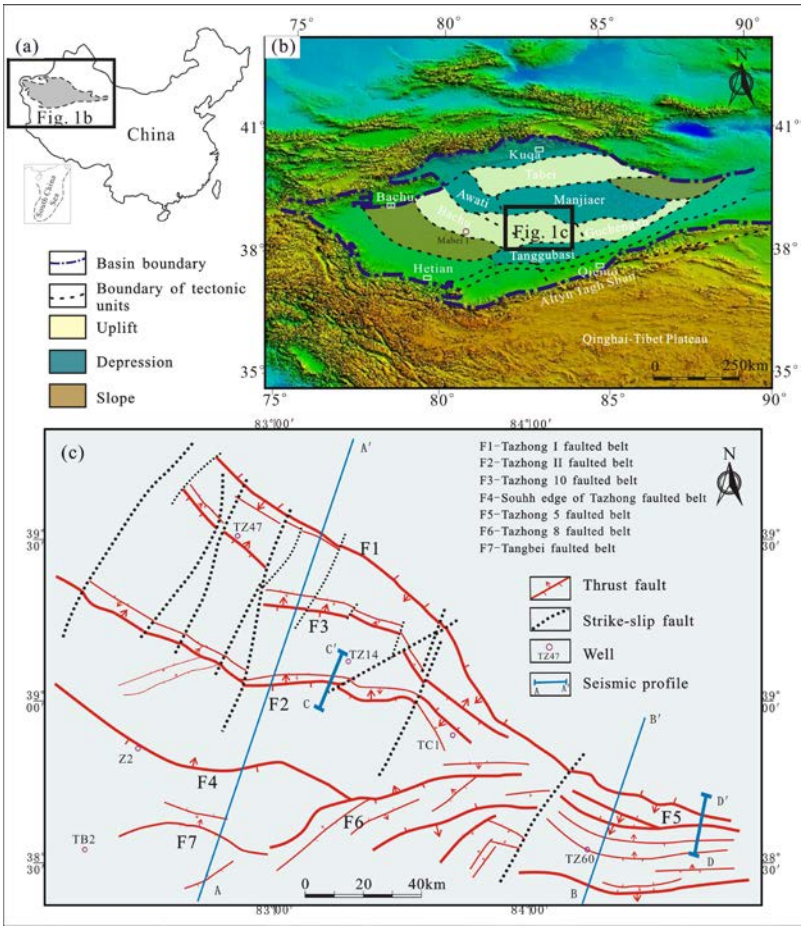

Figure 1. (a) Location of the Tarim Basin. (b) Map showing the distribution of tectonic units in the Tarim Basin. (c) Detailed map of the fault belts in the Tazhong area based on the interpretation of seismic data.

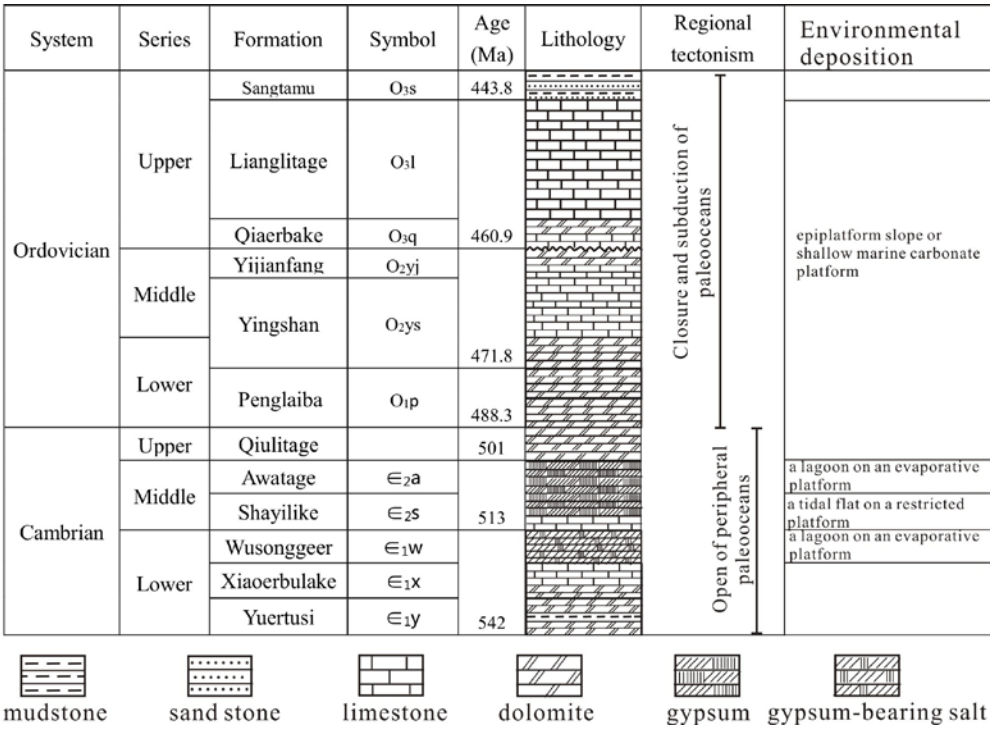

Figure 2. Schematic chart showing the Cambrian and Ordovician stratigraphy of the Tazhong area and timing of regional tectonic events

Only plant microfossils and algal stromatolites have been found. Well data from Mabei 1 suggested that

the lithology of the upper part of the Awatage Formation is dolomite, while the lower part is colorless, brown salt that is interbedded with sepia-colored mudstone, dolomitic mudstone and salty mudstone with a thickness ranging from 236 to 382 m. In terms of environmental deposition, this formation developed in a lagoon on an evaporative platform.

The Ordovician strata in the Tazhong uplift are primarily composed of carbonate platform deposits, except for the Upper Ordovician Sangtanmu Formation, which is mainly clastic in composition. The lower strata are carbonate deposits, which are in conformable contact with the Cambrian units. The Tazhong area was a NW-trending epiplatform slope or shallow marine carbonate platform from the Cambrian to the early Ordovician, and NE-trending dominantly extensional faults influenced later deformation processes. The Ordovician is the most intensely deformed layer in the Tazhong area. Due to the influence of the Mid-Caledonian movement, extensive faults and folds developed, which were then affected by Cambrian faults and formed complex differential interlayer deformation.

3. DIFFERENTIAL INTERLAYER DEFORMATION

The fault system in the Tazhong uplift is generally broom-like in plain view in that it diverges westward and converges eastward, as mentioned above (Fig. 1c). Combinations of fault structures are abundant in profile and can be clearly revealed in the geological cross section (Fig. 3), in which they appear as complex and variable features. Based on the combination characteristics of the fracture sections, the combined pattern of fractures in the Tazhong area shows a certain regularity and has obvious delamination differential structural deformation characteristics. In general, the pattern of the main faults in the geological cross section through the Tazhong area has typical "superimposed" deformation characteristics, indicating that the deep structure has a certain influence on the structural deformation of the middle and shallow layers, resulting in obvious structural coupling characteristics. "Superimposed" is a term generally used in basin that experienced multiphase structural event as a result of orogeny in the margin of the basin. In this article, however, it refer in particular to a complex structure formed by different fault styles overlapped vertically.

The "superimposed" fault combination in the Tazhong area can be divided into 5 styles: basal uplift+buried anticlinal fault block, basement normal fault+thrust fault (inverted type), basement fault+thickened gypsum salt rock+pop-up, buried uplifted fault block+drape anticline and magmatic diapir+associated faults, as shown in Table 1.

The basal uplift+buried anticlinal fault block is one of the main fault combination patterns in the Tazhong area and is mainly developed in the Tazhong 5 fault belt in the east. The deep layers of the Middle Cambrian unit and its underlying strata are mainly associated with positive tectonic units

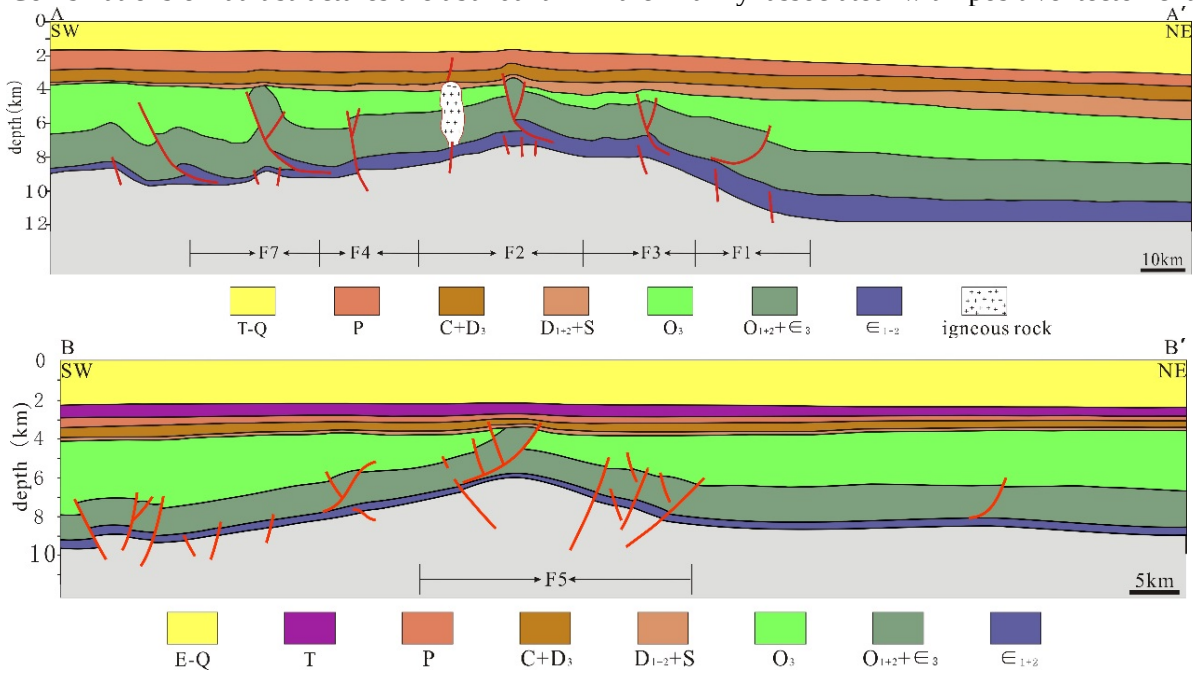

Figure 3. Geological cross sections in the Tazhong uplift showing characteristics of fault styles (see lines A-A' and B-B' in Fig. 1c for section location)

Table 1 Vertical structural coupling types and distribution in the Tazhong uplift

differential interlayer deformation types	Combination types of profile	Distribution
basement normal fault+thrust fault	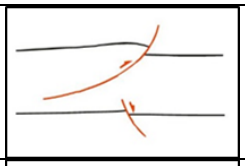	Tazhong I fault belt, South edge of Tazhong fault belt
basement fault+thickened gypsum salt rock+pop-up	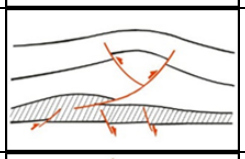	Tazhong II fault belt, Tazhong 10 fault belt
magmatic diapir+associated faults	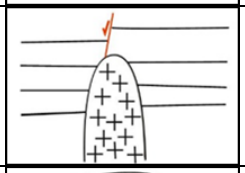	Tazhong II fault belt, Tazhong 10 fault belt
buried uplifted fault block+drape anticline	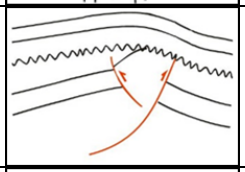	Tazhong 5 fault belt
basal uplift+buried anticlinal fault block	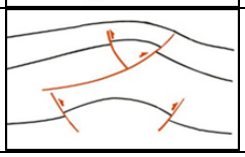	Tazhong 5 fault belt, Tazhong 8 fault belt

controlled by pop-up structures. The overlying main thrust faults slip off the top surface of the Middle Cambrian gypsum salt rock. There are also several rearward thrusts that form a pop-up structure. The development of this structure uplifted the strata gradually, which then experienced denudation, forming an unconformity that subsequently evolved into the buried uplifted fault block+drape anticline combination. The basement normal fault+thrust fault combination is mainly observed in the Tazhong I fault zone and is closely related to the east-west segmentation of the fault zone. The fault combination pattern has the characteristics of an inversion structure, reflecting the correlation of the upper and lower structural layers, which is a typical structural coupling phenomenon. In addition, it is also possible for the upper faults to overlap with the fault-related fold structure.

The combination of the basement fault+thickened gypsum salt rock+pop-up combination is most common in the Tazhong area, such as the No. II fault zone and the No. 10 fault zone in the high part of the Tazhong uplift.

Through detailed interpretation of the seismic section in areas where the Middle Cambrian gypsum salt rock has experienced plastic flow and is obviously thickened, the deep layer is found to have a certain degree of normal fault or reverse fault development, which indicates that the early basement fault has had a certain influence on the salt rock flow.

Furthermore, the plastic flow of the Middle Cambrian gypsum salt rock also controls the fault development in the overlying strata. The upper part of the overlying strata is pinched by the fault, which slips from the top of or inside the salt rock. The rearward thrusts in the hanging wall uplifted the fault block, which was then draped in sediment, forming a drape anticline; if this structural unit had been subjected to denudation, a typical buried uplifted fault block+drape anticline combination would have formed. In addition, the early faults also provided a channel for upwelling magma. The magma that upwelled into the shallow part formed magma diapirs, and the overlying strata were affected. Local extension occurred in the top stratum, and a small-scale normal fault are observed, thus forming the magmatic diapir+associated fault combination, such as that found in the Tazhong 47 area.

4. MECHANISM OF DEFORMATION

Previous studies have shown that preexisting basement structures exert great influence on the

deformation of overlying strata (Zhou et al., 2002, Tong et al., 2014; Bonini et al., 2016). Regions with different basement structures in the same area have different structural deformation behavior in the overlying stratum. The fault style in the Tazhong area is mainly controlled by the boundary conditions (including driving force and the orientation of the principal stress), basement structural features (including preexisting faults and paleo-uplifts), and development of the detachment layers. Furthermore, as evidenced by the results of the seismic profile interpretation, the style of shallow faults is closely related to the preexisting structures in the basement, the detachment layer properties and the regional tectonic evolution.

The existence of a detachment layer plays an important role in the development of reverse faults (Sepehr et al., 2006; Tang et al., 2008; Yan et al., 2008; Hume, 1987) and directly affects the structural deformation style of fold-and-thrust belts. As early as 1957, Hume (1987) proposed that faults may converge into one fault in deep incompetent strata and that the fault cuts through competent layers at depth. Incompetent strata are relatively weak layers that can act as detachment layers (Koyi & Vendevile, 2003; Massoli et al., 2006). Mossoli et al. (2006) used the sandbox model and confirmed that the styles of thrust fault belts are mainly controlled by the deep detachment layer and that fault-related structural combinations become more complicated with the participation of local shallow structures. Moreover, the deep detachment layer affects the structural deformation sequence and controls and constrains the deformation mechanism of the overlying strata at different depths.

4.1 Uniaxial rock mechanical test

A rock mechanical test can be used to determine the regional detachment layer. Previous studies (Gao et al., 2013, 2015; Li et al., 2001) have carried out rock mechanical tests in the Sichuan basin and the Tarim Basin. The results revealed a clear positive correlation between the uniaxial compressive strength and the Young's modulus of the rocks, and the contrast between competent layers and incompetent layers is distinct. Any of the rock mechanical parameters, such as compressive strength, Young's modulus and Poisson's ratio, can be used to predict the strong-weak relationship of the strata.

Rock samples were systematically collected from Ordovician carbonates and Cambrian gypsum in the Tazhong area. In the sampling process, efforts were made to avoid hidden fractures and fractures occurring during the sampling. According to international norms of rock mechanical analysis, the rock samples were made into cylinders with a height of 50 mm and a diameter of 25 mm. The rock mechanical tests were performed in the rock mechanical laboratory of the Southwest Petroleum University.

Parameters such as compressive strength (σc), Young's modulus (σc), and Poisson's ratio (μ) were measured to rule out the effects of Griffith cracks and end effects. The samples were tested more than 3 times. The Middle Cambrian to Ordovician strata have experienced intense deformation, and a clear difference is observed between the upper and lower rocks in terms of stratigraphic lithology, mechanical parameters and structural deformation characteristics (Table 2).

During the Cambrian period, the depositional environment of the Tazhong area was a shallow-water open platform (Tang et al., 2009. Gray and brown moderate to finely crystalline dolomite was deposited with algal dolomite, micritic limestone and calcareous mudstone. The Cambrian units are divided into the Yuertusi, Xiaoerbulake, Wusonggeer, Shayilike, Awatage and lower Qiulitage Formations from bottom to top, with a total thickness of 1600-2000 m and an unconformable contact with the underlying Sinian. The Middle Cambrian Awatage Formation and the Wusonggeer Formation contain thick gypsum layers, and the values of uniaxial compressive strength and density are 3.185~24.463 MPa and 2.0~2.2 g/cm3 (Table 2), respectively. These characteristics have an important influence on the fault development in the overlying Ordovician units in the uplift area of the Tazhong area. Apart from the structural high, where the Middle-Upper Ordovician units are absent over a large area and where the Lower Ordovician is partially absent, the Ordovician strata are relatively complete vertically and widely distributed in the Tazhong area. The Middle-Upper Ordovician strata are mainly composed of shallow water open platform deposits and are lithologically composed of gray black limestone, calcareous siltstone and dark shale with a thickness of 0-2300 m. However, the northern area of the Tazhong I fault belt is composed of trough-facies clastic sediments. The Ordovician limestone and underlying Middle Cambrian gypsum feature a conformable contact, although the average compressive strength and Young's modulus of the former are more than three times higher than those of the latter (Table 2).

Table 2. Result of rock mechanical tests

age	lithology	density (ρ)/g·cm^{-3}	uniaxial compressive strength (σ_c)/MPa	Young's modulus (E)/MPa	Poisson's ratio (μ)
$O_{1\text{-}2}y$	psammitic-micritic limestone	2.709	96.891	35.504	0.231
$O_{1\text{-}2}y$	gray micritic limestone	2.704	124.748	77.977	0.235
O_{1p}	dolomitic micritic limestone	2.715	94.543	85.061	0.279
$\in_{2a}$	white gypsum	2.196	26.463	18.585	0.317
$\in_{2a}$	white gypsum	2.035	3.185	5.926	0.205
$\in_{2a}$	white gypsum	2.173	24.549	22.613	0.276

4.2 Physical analog model

Many studies have focused on the mechanism of differential interlayer deformation (Horsfield, 1980; McClay & Scott, 1991; Tron & Brun, 1991; Koyi et al., 1993; Higgins & Harris, 1997; Bahroudi et al., 2003). The current understanding holds that the fault trend and the fault combination are mainly influenced by the lithologic properties of the basement (Dooley & McClay, 1997, McClay & Bonora, 2001), the geometric shape of the basin boundary (Dooley & McClay, 1997; Chemenda et al., 2002) and the extension direction (Mart & Dauteuil, 2000). A comparison of the rock mechanical parameters of the main deformation layers in the Tazhong area shows that the strengths of the Middle Cambrian and the overlying Ordovician are extremely different. Such a combination of lithologies has a certain influence on the mechanism of differential interlayer deformation.

To assess the characteristics of the differential interlayer deformation in the Tazhong area, two physical analog models were designed based on sandbox experiments. Different experimental results are obtained by changing different basement conditions. Based on these experiments, the influence of the basement structure on the differential interlayer deformation was analyzed.

4.2.1 Preexisting basement uplift model

The experimental apparatus is shown in figure 4. The basement paleo-uplift was simulated by arc-shaped polystyrene cystosepiment, above which a 0.5-cm-thick layer of silicone with a viscosity of 4.3×103 Pa·s was placed as a weak layer. A 4-cm-thick layer of silica sand was then placed over silicone to serve as the detachment layer. The total thickness of the silica sand and silicone was 4.5 cm. The left wall was moved at a constant speed of 3.3×10-5 m/s, and the total displacement was 15 cm. The right wall remained stationary, and photographs were taken throughout the experiment.

The final result of the experiment is shown in the figure 5. The fault, as a whole, was represented by an overstep propagation sequence, and thrust faults No. 1 and No. 2 converged in the ductile basement layer to form one fault (Fig. 5). When the displacement distance was 4 cm, just at the top of uplift, thrust fault No. 3 developed along the tangential direction of the paleo-uplift, and the fault also slipped in the ductile basement and exhibited a large fault throw. This experiment displayed the characteristics of fault evolution controlled by both the basement uplift and the detachment layer. When the displacement distance was 8 cm, backthrust fault No. 4 developed at the top of thrust No. 2, forming a "Y"-shaped fault combination. With increasing displacement distance, thrust fault No. 3 over the basement uplift had the largest fault throw.

The experimental results can explain the correlation of the fault development process under the control of the basal paleo-uplift and the detachment layer. Since the Late Cambrian, the collisional orogeny around the Tarim Basin has resulted in changes in the stress field. Seismic profiles show that there is an obvious basal paleo-uplift in the eastern part of the Tazhong area. For instance, the evolution of the Tazhong No. 5 fault is controlled by paleo-uplift. The Middle Cambrian ductile layer acts as a detachment layer during shallow fault development. The detachment layer has affected the development of faults in the Middle-Upper Ordovician strata.

The experimental results also demonstrate that a fault is more likely to develop along the tangential direction of an uplift and form a more complicated structural style if both a basement uplift and detachment layer are present.

The experimental process exhibits good similarity with the development model of the Tazhong 5 fault belt (Fig. 6). A pop-up structure-related uplift is observed in the seismic data, and faults associated with this uplift developed in the overlying Ordovician strata during the later fault evolution process. Similar to the fault development process, the combination of the upper and lower faults in the Tazhong 5 fault belt is constrained by

two factors: the basement structure and the detachment layer. Later compression transported the Upper Ordovician strata overlying the uplift upward along the fault plane, and the strata were then eroded, forming the current fault combination.

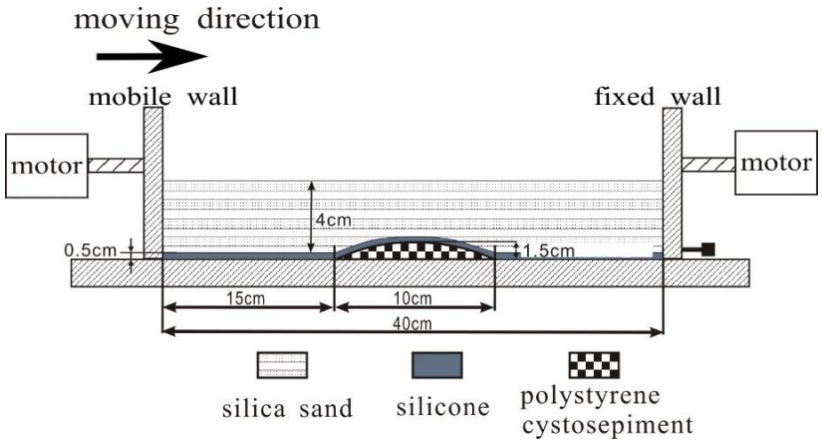

Figure 4 Experimental apparatus for the preexisting uplift (with decollement layer) model.

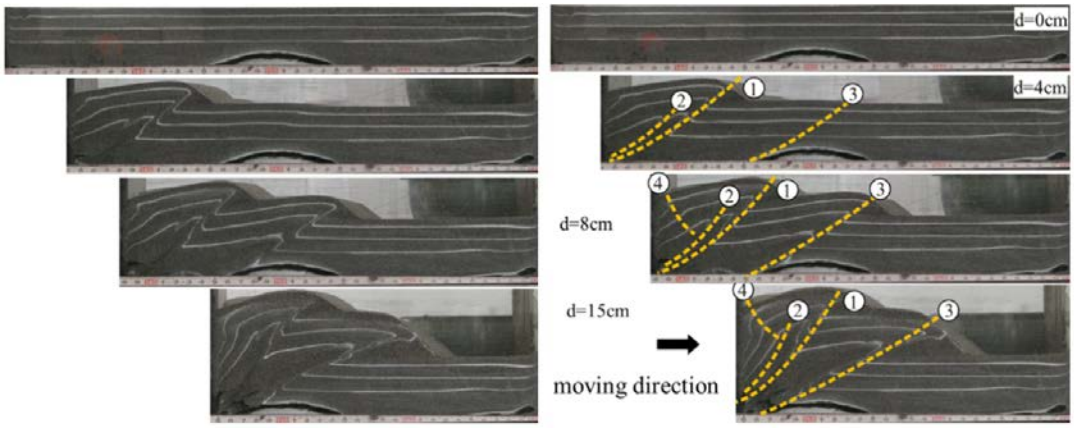

Figure 5 Fault development process in the preexisting uplift model (with decollement layer) where "d" is the moving distance, and the numbers indicate the development sequence of the faults.

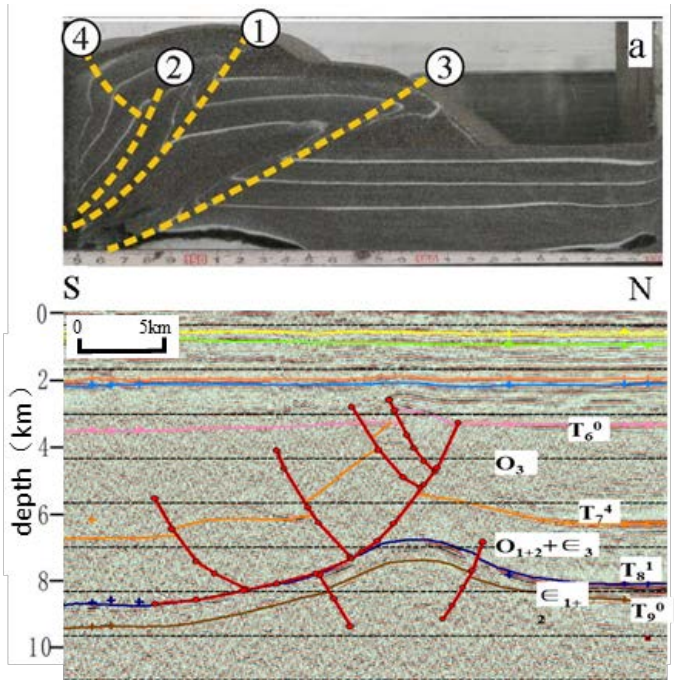

Figure 6. Comparisons of experimental results with seismic sections (see line C-C' in Fig. 1c for the section location)

4.2.2 Basement normal fault model

In the analog model, a basement normal fault was first rendered using silica sand at the bottom of the sandbox (Fig. 7). Then, directly above the normal fault, a 0.5-cm-thick silicone layer with the same properties as in the previous experiment was evenly deposited. Then, silica sand was deposited, achieving a total thickness of 6 cm for the silica sand and silicone together. To distinguish between the layers and the fault plane, white sand with the same physical properties as the gray sand was employed. The left wall was then propelled 10 cm towards the right wall at a constant speed of 3.3×10-5 m/s while the right wall remained still. Photographs were taken throughout the experiment.

The experimental results in figure 8 show the fracture combination characteristics under the joint influence of the basement normal fault and the detachment layer. When the compression distance was 2 cm, thrust fault No. 1 developed in front of the moving wall. This thrust fault had listric characteristics: the fault plane was steep in the upper part and gentle in the lower part where it slipped down along the soft layer. At a compression distance of 5.5 cm, fault throw on backthrust fault No. 2 was already obvious. Meanwhile, backthrust fault No. 3 developed in front of fault No. 1 and slipped down into the deep soft layer, forming a typical imbricated structure. With increasing compression distance, the most significant change was the development of thrust fault No. 4 right on top of the basement fault when the degree of shortening reached 20% (a movement distance of 8 cm). Because of the existence of a preexisting normal fault plane and detachment layer, the stress was concentrated above the normal fault instead of along the original normal fault plane, forming a type of inversion structure. When the compression distance reached 10 cm (a degree of shortening of 25%), the fault throw increased gradually, although the combination of fault styles did not change much. The throw on fault No. 4 increased, and backthrust fault No. 5 formed in the hanging wall of fault No. 4.

Similar to the previous experiment results, the existence of the basement normal fault makes it easier for later faults to develop in the vicinity, and the ductile layer provides the slip layer during the deformation process, which is conducive to the development of faults in overlying layers. Preexisting faults have strong selectivity in the later stage due to the switch in the stress field; some normal faults are inverted into reverse faults, and others retain their original properties. In our experiment, the detachment layer impeded the inversion of the preexisting normal fault; thus, a thrust fault developed over the basement normal fault. Based on a comparison of the experimental results with the actual seismic profile (Fig. 9), the two are found to have great similarity. A series of grabens and horsts caused by the extensional stress field in an earlier time period influenced the development of the later fault styles. The results of the analog experiment show that when the compressional distance reached a threshold of 8 cm (a shortening of 20%) in this model, the later faults developed above the basement normal fault because of the existence of the detachment layer and slipped down into this detachment layer. The experimental results explain the mechanism of differential interlayer deformation in the Tazhong area; that is, the complicated fault combination is the result of the combined effects of the basement structure and the detachment layer.

5. SIGNIFICANCE FOR HYDROCARBON GEOLOGY

Differential interlayer deformation in the Tazhong area presents a classical example of structural coupling. Complicated fault structures induced by multistage structural evolution exert considerable control over hydrocarbon accumulation (Mohammedyasin et al., 2016). As shown in this paper, the process of fault development not only directly impacts the development of structural traps and stratigraphic-lithologic traps but also influences the development of source rocks, reservoirs and hydrocarbon migration.

Furthermore, the properties and origins of hydrocarbons in different fault belts exhibit obvious differences (Xiang et al., 2010; Pang et al., 2013). The similarity shown in different parts of the same structural belt indicates that the hydrocarbons migrated primarily in the vertical direction through multistage faults, which serve as a major pathway for vertical migration. Numerous productive oil and gas fields in the Tazhong area are distributed along the fault belts because these faults act as vertical migration pathways for oil and gas and therefore play an important role in hydrocarbon accumulation and preservation.

Moreover, the unconformity above the Middle Ordovician strata contributes to the lateral migration of oil and gas. The widely developed multistage faults and large angular unconformities in the Tazhong area, especially areas exhibiting differential interlayer deformation associated with faults, are preferential migration pathways and serve as a three-dimensional network for vertical oil and gas migration. The complicated hydrocarbon migration and accumulation processes in the Tazhong area have been controlled by the superimposed hydrocarbon frameworks consisting of multiple layers vertically and multiple types of migration path horizontally.

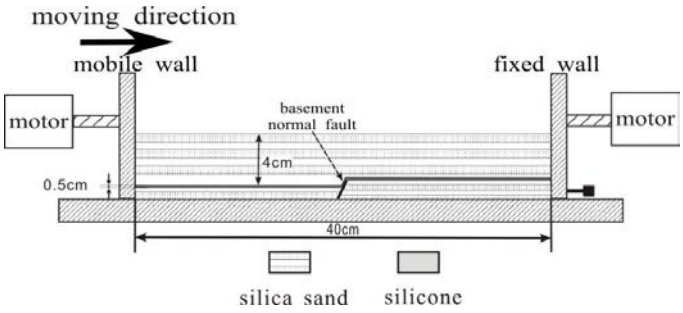

Figure 7. Experimental apparatus for a preexisting normal fault (with decollement)

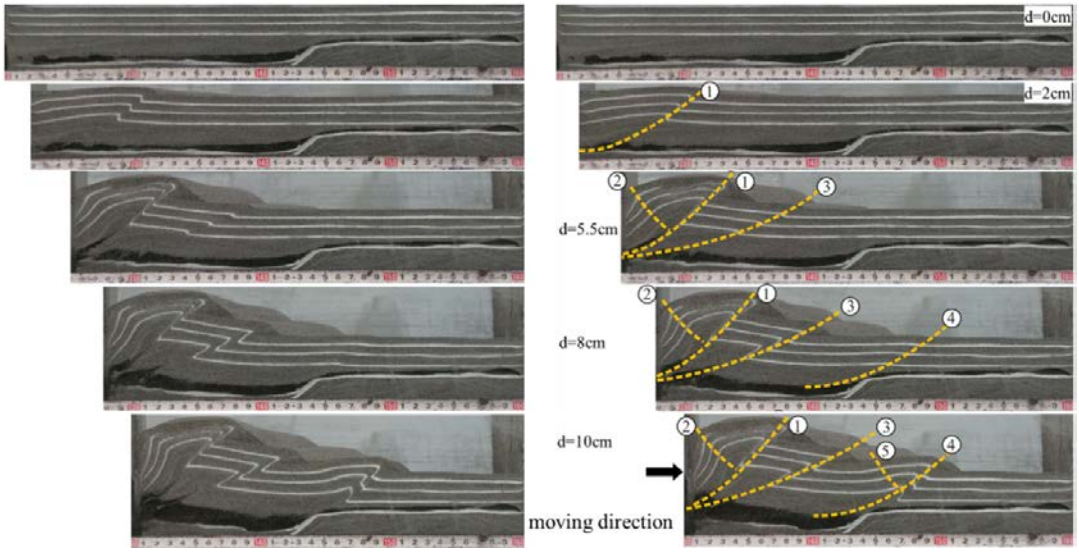

Figure 8 Faults development process with a preexisting normal fault (with decollement layer) model; d is the moving distance, and the numbers indicate the development sequence of the faults.

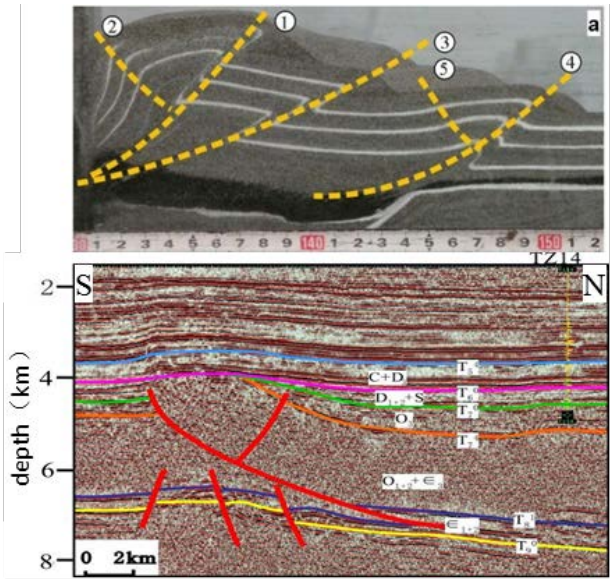

Figure 9 Comparisons of experimental results with seismic sections (see line D-D' in Fig. 1c for section location).

The faults are related and interact with each other in the Tazhong area and have exhibited activity during different geological stages. The existing vertical diversity also produces different types of hydrocarbon accumulation in the different fault belts because of their different effects on the upward process of oil and gas migration. This conclusion has also been successfully demonstrated by recent

exploration activities in the Tazhong area.

The Tazhong I fault belt simultaneously produces oil and gas, and the main productive layer is the Ordovician strata. In contrast, the main productive layer in the Tazhong 10 fault belt is the Silurian strata, from which only oil is produced. In the Tazhong II fault belt, the Carboniferous strata are the main productive layer. In general, from south to north, the main productive layers in the fault belts in the Tazhong area change from Carboniferous to Ordovician, and the layers bearing oil and gas reservoirs deepen. The differential interlayer deformation associated with faults is a double-edged sword for oil and gas accumulation. On the one hand, it facilitates the long-distance migration of deep oil and gas, which is then preserved in shallow strata; this aspect is conducive to oil and gas deposit development. On the other hand, multistage fault activity caused by differential interlayer deformation has a negative effect on hydrocarbon sealing. For instance, because many thrust faults developed in the southeastern Tazhong area in the Late Caledonian, the preservation conditions of oil and gas are poor due to natural gas leakage. Therefore, fault deformation-induced differences in the hydrocarbon accumulation in the fault belts in the Tazhong area indicate that different key hydrocarbon-bearing strata should be targeted in different fault beds with different deformational mechanisms.

6. CONCLUSION

The main conclusions are the next:

1) Differential interlayer deformation in the Tazhong area has clear structural coupling characteristics. In profile, the composite fault patterns can be divided into 5 types of “superimposed” faults. Deep structures and deformation in shallow strata have obvious relationships but weak correlations. The natural superimposition of multistage faults results in complex superimposed fault combinations.

2) The results of sandbox experiments revealed the mechanism of the differential interlayer deformation in the Tazhong area. The correlation between preexisting basement structures (the basement uplift and basement fault) and overlying faults is the main reason for such deformation. Because of the presence of the basement uplift, later faults form more easily in the area above the uplift. Likewise, the basement fault acts as a fracture plane that provides stress concentration points for the development of later thrust faults above the area with the preexisting fault, resulting in inversion structures.

3) The differential interlayer deformation of faults is a double-edged sword for oil and gas accumulation in the Tazhong area. On the one hand, it facilitates long-distance migration of deep oil and gas vertically through the development of multiple structural types in multiple layers and vertically superimposed traps resulting from the differential interlayer deformation of faults. On the other hand, the multistage activity of faults is detrimental to hydrocarbon preservation. Based on the differences in the patterns of oil and gas migration caused by differential interlayer deformation, different layers should be the focus of exploration in different fault belts due to differences in the formation mechanisms.

Acknowledgments

This study was funded by the National Natural Science Foundation of China (grant No. 41602158, 41972128), National Science and Technology Major Project (2017ZX05005-001-001) and the Strategic Priority Research Program of the Chinese Academy of Sciences (Grant No. XDZ14010101). We acknowledge the Northwest Company of Sinopec for providing the seismic profiles and allowing us to publish them.

References

Bahroudi, A., Koyi, H.A. & Talbot, C.J., 2003. *Effect of ductile and frictional decollement on style of extension.* J. Struct. Geol. 25, 1401-1423.

Bally, A. W., 1975. *A geodynamic scenario for hydrocarbon occurrences. Proceeding of Ninth World Petroleum Congress. Tokyo*: Tokyo Press, (1): 33-34.

Bashir, L., Gao, S. S. & Liu, K. H., 2013. *Crustal structure and evolution beneath the Colorado Plateau and the southern Basin and Range Province: Results from receiver function and gravity studies.* Geochemistry Geophysics Geosystems, 12(6): 231-255.

Beaumont, C., Fullsack, P. & Hamilton, J., 1992. *Erosional control of active compressional orogens.* Thrust Tectonics. 1-18

Bonini, L. Basili, R. Toscani, G. Burrato, P. Seno, S. & Valensise G., 2016. *The effects of pre-existing discontinuities on the surface expression of normal faults: Insights from wet-clay analog modeling.* Tectonophysics 684: 157-175.

Chemenda, A., Deverchere, J. & Calais, E., 2002. *Three-dimensional laboratory modelling of rifting: application to the Baikal Rift,* Russia Tectonophysics 356(4): 253-273.

Cruz, L., Malinski, J., Wilson, A., Take, W.A. & Hilley, G., 2010. *Erosional control of the kinematics and geometry of fold-and-thrust belts imaged in a physical and numerical sandbox.* J. Geophys. Res.115 (B09404), 1–15.

Cubas, N., Maillot, B. & Barnes, C., 2010. *Statistical analysis of an experimental com-pressional sand wedge.* J. Struct. Geol.32, 818–831.

Dooley, T. & McClay, K.R., 1997. *Analog modeling of pull-apart Basins.* AAPG Bull, 81(11). 1804-1826.

Graveleau, F., Malavielle, J. & Dominquez, S., 2012. *Experimental modelling of orogenic wedges: a review.* Tectonophysics, 538–540, 1–66.

Guan, S. W., Yang, H. J., Han, J. F., Li, B. L. & Luo, C. S., 2011. *Structural properties and interpretation methods of the Tazhong Low Salient.* Oil & Gas Geology 32(54), 777-786(in Chinese with English abstract).

Guo, L. Z., Zhu, W. B., Ma R. S., Sun, Y., & Wang, F., 2003. *Discuss on the structural coupling.* Geotectonica et Metallogenia, 27(3): 197-205 (in Chinese with English abstract).

Hall, J., 1815. *On the vertical position and convolutions of certain strata and their relationship with granite.* Trans. R. Soc. Edinb.7, 79–108.

Higgins, R. & Harris, L., 1997. *The effect of cover composition on extensional faulting above reactivated basement faults: results from analogue modelling.* J. Struct. Geol. 19 (1), 89-98.

Horsfield, W.T., 1980. *Contemporaneous movement along crossing conjugate normal faults.* J. Struct. Geol. 2 (3), 305-310.

Hsu, K. J., 1988. *Relic back-arc basins: Principles of recognition and possible new examples from China. In: kleinspehn K. L., Paola C. (Eds.), New Perspectives in Basin Analysis.* New York: Springer-Verlag, 245-263.

Hume, G S. 1987. *Fault structures in the foothills and eastern Rocky Mountains of Southern Alberta*. Geological Society of America Bulletin 68(10): 395-412.

Jin, Z. J., 2005. *New advancement in research of China's typical superimposed basins and reservoiring (Part I): Classification and research methods of superimposed basins.* Oil & Gas Geology, 26 (5), 553-562 (in Chinese with English abstract).

Kay, R. W. & Mahlburg, Kay, S., 1993. *Delamination and delamination magmatism. In: Green, A. G., Kröner, A., Götze, H. J., Pavlenkova, N. (Eds.), Plate Tectonic Signatures in the Continental lithosphere.* Tectonophysics, 219: 177-189.

Kim, Y.-S. & Sanderson, D.J., 2005. *The relationship between displacement and length of faults: a review.* Earth Sci. Rev. 68, 317-334.

Klein, G. V., 1987. *Current aspects of basin analysis.* Sedimentary Geology. 15: 95-118.

Koyi, H., Jenyon, M.K. & Petersen, K., 1993. *The effect of basement faulting on diapirism.* J. Petroleum Geol. 16 (3), 285-312.

Koyi H., &Vendevile B., 2003. *The effect of decollement dip on geometry and kinematics of model accretionary wedges.* Journal of Structural Geology 25: 1445-1450.

Li, B. L., Sun, Y., Zhu, W. B., Guo, J. C. & Wen, S. H., 2001. *Study on the layer slip parameter systems in the eastern Sichuan.* Journal of Southwest Petroleum Institute 23(1): 29-33.

Li, C. X., Jia, C. Z., Li, B. L., Yang, G., Yang, H. J., Luo, C. S., Han, J. F. & Wang, X. F., 2009. *Distribution and Tectonic Evolution of the Paleozoic Fault System, the North Slope of Tazhong Uplift, Tarim Basin.* Acta Geologica Sinica 83(8), 1065-1073(in Chinese with English abstract).

Li, C. X., Wang, X. F., Li, B. L. & He, D. F., 2013. Paleozoic fault systems of the Tazhong Uplift, Tarim Basin, China. Marine and Petroleum Geology 39(1): 48-58.

Li, J. L., Xiao, W. J. & Yan, Z., 2003. *Basin-range coupling and its sedimentation.* Acta Sedimentologica Sinica, 21(1): 52-60.

Li, Y. J., Wu, G. Y., Meng, Q. L., Yang, H. J., Han, J. F., Li, X. S. & Dong, L. S., 2008. *Fault systems in central area of the Tarim Basin: geometry, kinematics and dynamic settings.* Chinese Journal of Geology (Scientia Geologica Sinica) 43 (1), 82-118(in Chinese with English abstract).

Mart, Y. & Dauteuil, O., 2000. *Analogue experiments of propagation of oblique rifts.* Tectonophysics 316(1~2): 121-132.

Massoli, D., Koyi, H. A. & Barchi, M. R., 2006. *Structural evolution of a fold and thrust belt generated by multiple décollements: analogue models and natural examples from the Northern Apennines (Italy).* Journal of Structural Geology 28(2): 185-199.

McClay, K.R. & Bonora, M., 2001. *Analogue experiments of restraining stepovers in strike-slip fault system* AAPG Bull. 2001, 85(2): 233-260.

McClay, K.R. & Scott, A.D., 1991. *Experimental models of hanging wall deformation in ramp-flat listric extensional fault systems.* Tectonophysics 188, 85-96.

Mohammedyasin, S. M., Lippard, S. J., Omasanya, K. O., Johansen S. E. & Harishidayat D., 2016. *Deep-seated faults and hydrocarbon leakage in the Snøhvit Gas Field, Hammerfest Basin, Southwestern Barents Sea.* Marine and Petroleum Geology 77: 160-178.

Nieuwland, D.A., Urai, J.L. & Knoop, M., 2001. *In-situ stress measurements in model experiments of tectonic faulting. In: Lehner, F.K., Urai, J.L. (Eds.),* Aspects of Tec-tonic Faulting. Springer-Verlag, pp.155–167.

Pang, H., Chen, J. Q., Pang, X. Q., Liu, K. Y., Liu, L. F., Xiang, C. F. & Li, S. M., 2013. *Analysis of secondary migration of hydrocarbons in the Ordovician carbonate reservoirs in the Tazhong uplift, Tarim Basin, China*. AAPG Bulletin 97, 1765-1783.

Liu, L., Kang, L., Cao, Y. T., Yang, W., Q., 2015. *Early Paleozoic granitic magmatism related to the processes from subduction to collision in South Altyn, NW China. Science China Earth Science* 58, 1513-1522.

Schlische, R.W., Young, S.S., Ackermann, R.V. & Gupta, A., 1996. *Geometry and scaling relations of a population of very small rift-related normal*

faults. Geology 24, 683-686.

Sepehr, M., Cosgrove, J. & Moieni, M., 2006. *The impact of cover rock rheology on the style of folding in the Zagros fold-thrust belt.* Tectonophysics 427(1-4): 265-281.

Souloumiac, P., Maillot, B. & Leroy, Y.M., 2012. Bias due to side wall friction in sand box experiments. J. Struct. Geol.35, 90–101.

Gao, L. H., Han, Z. Z., Han, Y., Han, C., Wei, F. F., Qin,Z., 2013. *Controlling of cements and physical property of sandstone by fault as observed in well Xia503 of Huimin sag, Linnan sub-depression. Science China Earth Sciences* 56, 1942-1952.

Gao, K. D., Du, C. L., Dong, J. H., Zeng, Q. L., 2015. *Influence of the Drum Position Parameters and the Ranging Arm Thickness on the Coal Loading Performance. Minerals* 5, 723-736.

Tang, L. J., Yang K. M., Jin W. Z., Lv, Z. Z. & Yu, Y. X., 2008. *Multi-layers and decollement deformation in Longmen Mountain thrust belt.* Science in China (Series D: Earth Sciences) 38(S1): 30-40(in Chinese with English abstract).

Tang, L. J., Huang, T. Z., Jin, W. Z., Lv, Z. Z., He, C. B., Ning, F., Wang, P. H. & Chen, Q., 2009. *Differential deformation and hydrocarbon accumulation in the superimposed basins.* Earth Science Frontiers, 16(4), 013-022 (in Chinese with English abstract).

Tong, H. M., Koyi, H., Huang, S. & Zhao, H., 2014. *The effect of multiple pre-existing weaknesses on formation and evolution of faults in extended sandbox models.* Tectonophysics 626: 197-212.

Tron, V. & Brun J. P., 1991. *Experiments on oblique rifting in brittle-ductile systems.* Tectonophysics 188, 71-84.

Uydea, S., 1983. *Comparative subductology.* Episodes. 2: 19-34.

Wu, G. H., Yang, H. J., Qu, T. L., Li, H. W., Luo, C. S. & Li, B. L., 2012. *The fault system characteristics and its controlling roles on marine carbonate hydrocarbon in the Central uplift, Tarim Basin.* Acta Petrologica Sinica 28(3), 793-805(in Chinese with English abstract).

Xiang, C. F., Pang, X. Q. & Yang, W. J., 2010. *Hydrocarbon migration and accumulation along the fault intersection zone: A case study on the reef-flat systems of the No. 1 slope break zone in the Tazhong area, Tarim Basin.* Petroleum Science 7, 211-225.

Xiao, X. M., Song, Z. G., Liu, D. H., Liu, Z. F., & Fu, J. M., 2000. *The Tazhong hybrid petroleum system, Tarim Basin.* Marine and Petroleum Geology 17, 1-12.

Yan, D. P., Jin, Z. L., Zhang, W. C. & Liu, S. F., 2008. *Rock mechanical characteristics of the multi-layer detachment fault system and their controls on the structural deformation style of the Sichuan-Chongqing-Hunan-Hubei thin-skinned belt, South China.* Geological Bulletin of China 27(10): 1687-1697(in Chinese with English abstract).

Yang, H. J., Wu, G. H. & Han, J. F., 2007, *Characteristics of hydrocarbon enrichment along the Ordovician carbonate platform margin in the central uplift of Tarim Basin.* Acta Petrolei Scinica 28, 26-30(in Chinese with English abstract).

Yang, S. B., Liu, J., Li, H. L., Zhang, Z. P. & Li, J. J., 2013. *Characteristics of the NE-trending strike-slip fault system and its control on oil accumulation in north pericline area of the Tazhong paleo uplift.* Oil & Gas Geology 34(6), 797-802(in Chinese with English abstract).

Yu, Y. X., Huang, T. Z., Tang, L. J., Chen, X. Y. & Cui, Z. H., 2010. *Internal Structural Deformation of the Tazhong Lower Uplift, Tarim Basin.* Geoscience 24(6), 1029-1034(in Chinese with English abstract).

Zhang, Z. S., Li, M. J. & Liu, S. P., 2002. *Generation and evolution of Tazhong low uplift.* Petroleum Exploration and Development 29(1): 28-31(in Chinese with English abstract).

Zhou, J. X., Wei C. G. & Zhu Z. J., 2002. *Influence of substrate Contraction on the deformational characteristics of compressional structures: Insight from sandbox experiments.* Earth Science Frontiers 9(4): 377-382(in Chinese with English abstract)

Received at: 09. 08. 2019
Revised at: 14. 10. 2019
Accepted for publication at: 07. 01. 2020
Published online at: 15. 01. 2020